UC Davis
UC Davis Previously Published Works

Title

Generation of a Novel Rat Model of Angelman Syndrome with a Complete Ube3a Gene Deletion.

Permalink

https://escholarship.org/uc/item/36d5z4xk

Journal

Autism research : official journal of the International Society for Autism Research, 13(3)

ISSN

1939-3792

Authors

Dodge, Andie
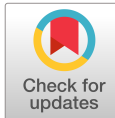Peters, Melinda M
Greene, Hayden E
et al.

Publication Date

2020-03-01

DOI

10.1002/aur.2267

Peer reviewed

RESEARCH ARTICLE

Generation of a Novel Rat Model of Angelman Syndrome with a Complete *Ube3a* Gene Deletion

Andie Dodge,* Melinda M. Peters,* Hayden E. Greene, Clifton Dietrick, Robert Botelho, Diana Chung, Jonathan Willman, Austin W. Nenninger, Stephanie Ciarlone, Siddharth G. Kamath, Pavel Houdek, Alena Sumová, Anne E. Anderson, Scott V. Dindot, Elizabeth L. Berg, Henriette O'Geen, David J. Segal, Jill L. Silverman, Edwin J. Weeber, and Kevin R. Nash

Angelman syndrome (AS) is a rare genetic disorder characterized by severe intellectual disability, seizures, lack of speech, and ataxia. The gene responsible for AS was identified as *Ube3a* and it encodes for E6AP, an E3 ubiquitin ligase. Currently, there is very little known about E6AP's mechanism of action *in vivo* or how the lack of this protein in neurons may contribute to the AS phenotype. Elucidating the mechanistic action of E6AP would enhance our understanding of AS and drive current research into new avenues that could lead to novel therapeutic approaches that target E6AP's various functions. To facilitate the study of AS, we have generated a novel rat model in which we deleted the rat *Ube3a* gene using CRISPR. The AS rat phenotypically mirrors human AS with loss of Ube3a expression in the brain and deficits in motor coordination as well as learning and memory. This model offers a new avenue for the study of AS. ***Autism Res 2020, 00: 1–13.*** © 2020 International Society for Autism Research, Wiley Periodicals, Inc.

Lay Summary: Angelman syndrome (AS) is a rare genetic disorder characterized by severe intellectual disability, seizures, difficulty speaking, and ataxia. The gene responsible for AS was identified as *UBE3A*, yet very little is known about its function *in vivo* or how the lack of this protein in neurons may contribute to the AS phenotype. To facilitate the study of AS, we have generated a novel rat model in which we deleted the rat *Ube3a* gene using CRISPR. The AS rat mirrors human AS with loss of *Ube3a* expression in the brain and deficits in motor coordination as well as learning and memory. This model offers a new avenue for the study of AS.

Introduction

Angelman syndrome (AS) is a rare neurogenetic disorder caused primarily by alterations within the maternally inherited allele for *UBE3A*, encoding for an E3 ubiquitin ligase. *UBE3A* undergoes neuron-specific imprinting, which transcriptionally silences the paternal allele with an antisense transcript. This results in predominant maternal *UBE3A* expression within the brain [Meng, Person, & Beaudet, 2012]. Maternal disruption of *UBE3A* results in a >95% reduction of neuronal UBE3A protein within the CNS leading to the manifestation of AS symptoms. In peripheral tissue, there is biallelic expression of *UBE3A*, with a >50% reduction of protein expression in AS patients [Gustin et al., 2010].

Angelman syndrome is characterized by severe cognitive and motor deficits, seizures, abnormal EEGs, speech impairments, sleep disturbances, and a generally happy demeanor [Williams, Driscoll, & Dagli, 2010]. Approximately 70% of AS patients have a genetic alteration comprised of a *de novo* deletion within 15q11–q13 on the maternal chromosome. Additionally, *UBE3A* expression may be reduced by other mechanisms such as imprinting defects of the maternal copy (~6%), paternal uniparental disomy (~3%), and mutations within the maternal chromosome (~13%), all of which can lead to AS development [Y. Jiang, Lev-Lehman, Bressler, Tsai, & Beaudet, 1999; Lalande & Calciano, 2007]. Despite the profound and penetrant symptoms in AS, there are no gross anatomical aberrations noted in either the AS human brain or the

current AS mouse model brain [Bird, 2014; Judson et al., 2017; Williams et al., 2006; Williams et al., 2010].

Much of what is known about the AS condition is from studies conducted on the murine model [Y. H. Jiang et al., 1998]. The AS mouse model, produced through an exon 2 null mutation, has supported molecular research and refined drug discovery since its introduction two decades ago [Y. H. Jiang et al., 1998]. While this model is widely used and reported, there are notable challenges including, but not limited to, strain influences and phenotypic inconsistency [Born et al., 2017; Huang et al., 2013]. This has led to interest in the generation of new models for AS which could more closely reflect the human AS phenotype.

Traditionally, rats have offered a more preferable model of human disorders due to greater similarities in human physiology. Rats, in general, have a much larger brain and body size facilitating the utilization of a wider array of cognitive, social, and biochemical techniques [Ellenbroek & Youn, 2016; Iannaccone & Jacob, 2009; Kummer et al., 2014]. A larger size will also aid in facilitating some detailed developmental, anatomical, and physiological measurements which are not as feasible in mice due to its smaller size. Rats have been highly characterized and exhibit higher motor coordination and behavioral complexity, giving a more accurate assessment of cognitive outcomes especially during a developmental time course [Ellenbroek & Youn, 2016; Iannaccone & Jacob, 2009; Kummer et al., 2014]. Within the pharmaceutical industry it has become standardized to use the rat for a physiological and toxicological model [Parasuraman, 2011]. Thus, the use of a rat AS model may allow researchers to better understand the AS condition and permit a more accurate assessment of novel therapeutic approaches in a superior model of AS.

As mentioned previously, the majority of human AS cases arise from a large deletion of the maternal *UBE3A* gene. The previous AS mouse model is limited to a 3 kb sequence deletion, including exon 2, resulting in a deletion of 100 N-terminal amino acids of *UBE3A* and a frameshift inactivating all putative protein isoforms, which does not reflect the majority of human AS manifestation [Y. H. Jiang et al., 1998]. Therefore, we set out to produce a novel rat AS model which would encompass a deletion of the entire *Ube3a* gene. In conjunction with this genetic alteration, the higher complexity of the rat brain would allow for a refinement of a modeled AS phenotype to better resemble the human condition.

Here, we report the generation of this novel rat model using CRISPR technology. We compare the maternal gene knockout rat to its wild-type littermates, evaluating *Ube3a* expression within the brain. We observed that there are no gross anatomical aberrations within the brain structures. Western blotting indicates decreased *Ube3a* expression within the brain, recapitulating what has been displayed in the AS mouse model. General motor coordination, gait alterations, sociability, and memory deficits were characterized in this novel model.

Materials and Methods
Animals

CRISPR Cas 9 technique was used to generate a full deletion of the rat *Ube3a* gene with ~90 kb deletion. This was performed at Transposagen (Lexington, KY). Four CRISPR guide RNAs were designed: 5′ CRISPR-1 target site GG CCCTGCAGAGATGCAATC, 5′ CRISPR-2 target site GGA GCCCTCCGCCGGCA, 3′ CRISPR-1 target site TACCC TTCCCAGGCCCC; 3′ CRISPR-2 target site GCATTTC TAGTACATCATCC; two each to areas that flank the entire *Ube3a* region. A vector that contained arms of homology that spanned the region to be deleted was also included in the hopes that it may facilitate the deletion (this did not get incorporated into the final clone). Almost 200 Sprague–Dawley embryos were injected (in two separate cohorts) which resulted in 11 births. Animals were screened with the primers Ube3aDelF1 (AACACCAAGCCTCTCTCAGC) and Ube3aDelR1 (ACCAGGCCTCAAAATTGACA) and two pups were identified as positive for the deletion. These were then rescreened with Ub3aDelSpcfcF4 (ACATGGCTCTAAAAG AGTTCAGG) and Ube3aDelR1. Analysis of the region deleted (~90 kb) is shown in Figure 1 and corresponds with CRISPR target 1 deletion.

DNA for genotyping was extracted from ear tissue using an alkaline lysis reagent (10 N NaOH, 0.5 M EDTA, pH 12). The sample was heated to 95°C for 30 min followed by the addition of a neutralization buffer (40 mM Tris–HCl, pH 5). Initial genotyping screening was performed using the following primers: for AS Ube3aDelSpcfcF6 [ACCTAGCCCAAAG CCATCTC] (0.4 μM) and Ube3DelR2 [GGGAACAGCAAAAG ACATGG] (0.4 μM) which generates a 917 bp product; and for wild-type Rube1123 [TAGTGCTGAGGCACTGGTTCAG AGC] (0.4 μM) and Rube1606r [TGCAAGGGGTAG CTTACTCATAGC] (0.4 μM) which generates a 459 bp product. Cycling at 95°C for 30 sec/59°C for 45 s/72°C for 1.5 min with 35 cycles. Results are shown in Figure 1B. To reconfirm initial genotyping results, additional primer pairs were designed. This pair produced a smaller PCR product increasing accuracy with high fidelity. An alternative set of genotype primers was designed to reduce the product size for the deletion to 232 bp and to increase product efficiency and reproducibility, using Ube3aDelSpcfcF6 and AS-RR2 (TATTTTCCCCACCAAACACC; 0.4 μM). In this genotyping, the wild type primers were included at 0.48 μM and the cycles performed as above.

Breeding Strategy

Ube3a deletion founder rats were backcrossed with Sprague–Dawley rats for each generation. Original male founder rats were bred to obtain paternal deletion
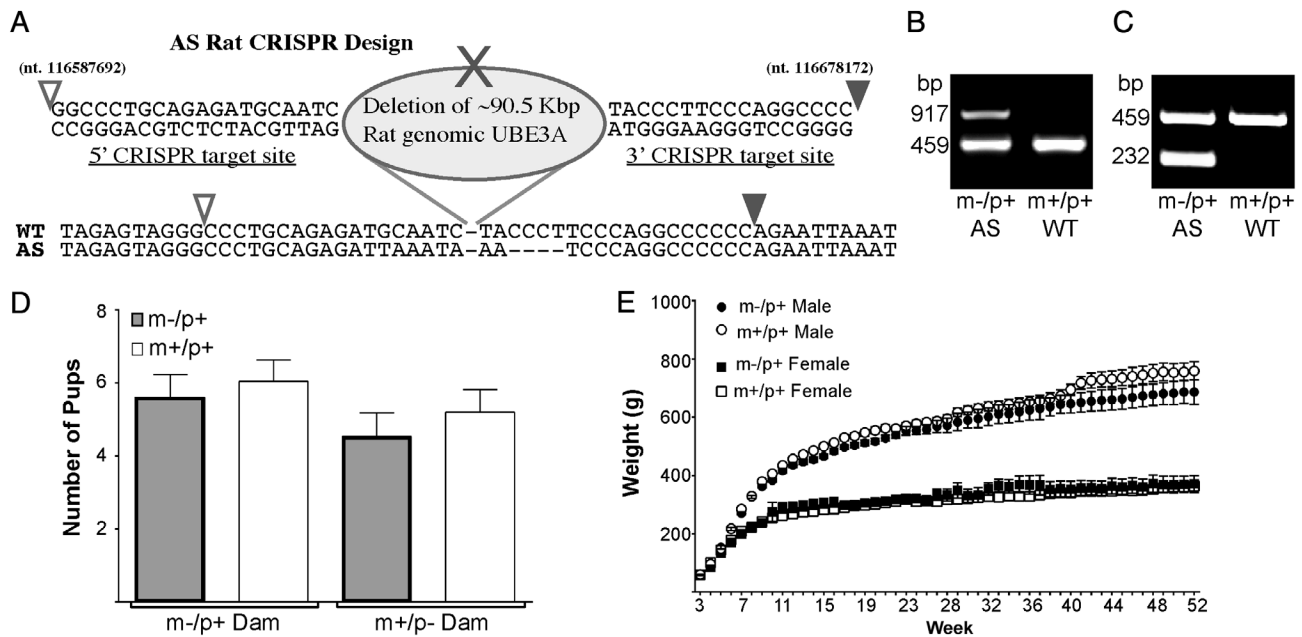
Figure 1. (A) Schematic of the *Ube3a* gene deletion including target sites for the CRISPR guide RNA's and actual sequence of the gene region below. Open arrowhead represents nucleotide sequence number 116587692 and the closed arrow represents nucleotide 116678172 of the rat chromosome 1 (NCBI Ref. Seq.: NC_005100.4). (B) Representative image of PCR results from primers used in initial genotype screening generates a ~900 bp band for the AS deletion. Samples positive for the full deletion alongside a WT control group are shown (WT primers generate a ~450 bp band). (C) Representative image of additional genotyping PCR with results for the AS full deletion (232 bp) alongside a WT control group. (D) Normal litter size and Mendelian distribution is seen regardless of whether the dam had a paternal or maternal deletion for *Ube3a* (Paternal deletion dam, $n = 24$; Maternal deletion dam $n = 15$). (E) Weights measured every week up to 1 year of age. When compared to WT (m+/p+) littermate controls $n = 18$ (10M, 8F), AS (m−/p+) rats $n = 11$ (6M, 5F) do not have a significant difference in weight-based upon sex.

offspring. Female offspring carrying the *Ube3a* deletion were then bred with Sprague–Dawley males to produce maternal deletion offspring for experiments. No differences were seen in litter sizes and genotypes if the dam had a paternal deletion or maternal deletion. Therefore, maternal deletion females can be used for breeding unlike the AS mouse where typically a paternal line is maintained for generation of AS animals. Maternal breeding was used to generate the animals used in this study. Animals were housed in a standard 12-hr light/dark cycle and supplied with food and water *ad libitum* at the University of South Florida, and were housed in groups of two per cage. All procedures were conducted in compliance with the NIH Guidelines for the Care and Use of Laboratory Animals and approved by the Institutional Animal Care and Use Committee of USF (approval number A4100-01).

Western Blotting

Tissue samples were collected directly following rapid decapitation. Followed by homogenization with (1:100) dilution of mammalian M-PER (Millipore) supplemented with (1×) phosphatase and (1×) protease inhibitors (Thermo Scientific). Protein concentration was measured using BCA Protein Assay Kit (Thermo Scientific) and standardized to BSA.

Laemmli buffer (Bio-Rad) and equal amounts of protein (3 μg) were loaded into 15 well SDS-PAGE gel (10%). After transferring the gels onto PVDF transfer membranes (Bio-Rad), blots were incubated at room temperature in Revert total protein stain (Li-Cor Biosciences) for 5 min following by 2 × 3 min incubations in revert wash buffer. The revert was imaged and quantitated on the Odyssey scanner. Blots were blocked in 1× Tris-buffered saline with 0.1% Tween 20 (Sigma-Aldrich), and 5% nonfat dry milk (Lab Scientific) at room temperature ($23 \pm 2\,^{\circ}\mathrm{C}$) for 2 hr. The blots were then incubated in primary antibody, rat Ube3a (Millipore, 1:10,000) diluted in 5% nonfat dry milk mixed in Tris-buffered saline with 0.1% Tween 20 and left overnight at $4\,^{\circ}\mathrm{C}$. After incubation, blots went into three 10-min washes in Tris-buffered saline with 0.1% Tween 20. The blots were then incubated with goat anti-rabbit IgG-800CW (Li-Cor Biosciences) at 1:10,000. Membranes then went into three 10-min rinses, as previously mentioned and were detected and analyzed using the Li-Cor Odyssey and software. Individual T-tests were used to analyze for significance.

Immunohistochemistry

Rats ($n = 10$) were deeply anesthetized with Somnasol and perfused with PBS (0.01 M sodium phosphate–

0.15 M NaCl, pH 7.2) and then freshly prepared 4% para-formaldehyde in PBS. Brains were post-fixed for 12 hr at 4°C and cryoprotected in 30% sucrose in PBS for shipping to Dr Sumová. Coronal 30 μm-thick sections were cut and processed for free-floating immunohistochemistry using the standard avidin-biotin method with diaminobenzidine (Vector Laboratories, Peterborough, UK) as previously described [Sumova, Sladek, Jac, & Illnerova, 2002]. The anti-Ube3a mouse monoclonal antibody (Sigma, SAB1405408) was used as the primary antiserum (1:600). The sections of both genotypes were processed within one assay and all sections were developed in diaminobenzidine for exactly the same time.

Functional Observational Battery

Home cage behavior was monitored using a modified functional observational battery (FOB) from Moser and MacPhail [1992]. First, rats were observed in their home cage for 60 sec and behavior measurements recorded (posture, palpebral closure, convulsions or tremors, biting, and vocalization). Next, rats were moved to a clean cage containing a mark to indicate the midline of the cage and singly housed for 10 min. Responses to handling were recorded (ease of removal from cage, ease of handling, fur appearance). During the 10 min, total number of crosses between sides, piloerection, number of audible vocalizations (not ultrasonic), grooming episodes, eating episodes, drinking episodes, fecal bolus number, and urine spot number were measured.

Weight measurements involved male and female animals were weighed every 7 days starting from the day of being weaned (day 21 post-natal) until 1 year of age (WT $n = 18$, AS $n = 11$). It should be noted that 32 WT and 20 AS rats began weight measurement at PND 21. Fourteen WT and nine AS rats were removed for other research purposes before week 52. These other animals matched the weights of those shown in the graph up until they were euthanized.

Behavioral Testing Cohorts

All behavior testing occurred in the adult rats aged 3–4 months. Four cohorts of animals were used. Cohort 1: DigiGait, hind-limb clasping, and novel object; Cohort 2: light/dark, y-maze, social approach, novel object, and fear conditioning; Cohort 3: rotarod, open field, elevated plus maze, y-maze, and fear conditioning; Cohort 4: open field, elevated plus maze, and y-maze. Animals used in this study were F3–F5 generation from founders.

Hind Limb Clasping

Hind limb clasping was used as a marker for neurological dysfunction and evaluated hind limb response to being suspended approximately 10 cm above a smooth surface.

Suspension was recorded by video camera for post-testing analysis, which was performed by a separate technician, blinded to animal genotypes. A scoring system ranged between 0 and 3. If assigned a0, the animal consistently kept legs away from abdomen splaying outward, considered typical hind limb posture. If assigned a1, the animal consistently retracted a single leg toward the abdomen or in a rigid upward movement while the other splayed outward. If assigned a2, the animal partially retracted both hind limbs toward the abdomen. If assigned a3, both hind limbs were entirely retracted touching the abdomen or touching one another. All weanling animals were tested 21 days post-natal (AS $n = 69$ (30F, 39M), WT $n = 90$ (45F, 45M)) and a subset of animals that underwent behavior testing were tested again at 4–5 months post-natal (AS $n = 16$ (8M, 8F), WT $n = 18$ (10M, 8F). An independent t-test was used to analyze data.

Rotarod

General motor coordination and stamina were tested using the rotorod. Animals were placed on a 7 cm diameter rotarod (Ugo Basile). The rod accelerated from 4 to 40 rpm over a 5-min time period. Rats were recorded for latency to fall off of the rotating rod over a 2-day period with four trials each day, each trial separated by 30 min (3–4 months of age, AS $n = 10$ (5F, 5M), WT $n = 10$ (5F, 5M)). A repeated measures ANOVA was used to analyze data.

DigiGait

Gait analysis was performed on a DigiGait (Mouse Specifics, Inc.) at a speed of 15 cm/sec. Rats were acclimated to an enclosed translucent treadmill before initiation of the belt. Animals were typically recorded for less than 60 sec, to achieve at least 3 sec of clearly recorded, consecutive steps. Gait analysis was analyzed using the DigiGait program. Rats were 3–4 months of age with AS $n = 20$ (11F, 9M) and WT $n = 18$ (8F, 10M). An independent t-test was used to analyze data.

Open Field

The open field is used as a standard test of general activity. Animals are monitored for 15 min in a 60 cm square open field with a video tracking software (Noldus), under moderate lighting (3–4 months of age, AS male $n = 8$, AS female $n = 8$, WT male $n = 8$, WT female $n = 8$). General activity levels were evaluated by Ethovision XT software (Noldus). An independent t-test was used to analyze data.

Light/Dark

Light/dark was conducted by placing the animal (3–4 months, AS $n = 14$, WT $n = 12$) in a two-chambered apparatus for 15 min, recording the total time spent in the

light (40 by 30 cm) and dark side (40 by 22 cm), as well as total distance traveled and number of entries into the light chamber (Ethovision XT, Noldus). An independent *t*-test was used to analyze data.

Elevated Plus Maze

Rats (3–4 months, AS male *n* = 8, AS female *n* = 8, WT male *n* = 8, WT female *n* = 8) were placed in elevated plus maze apparatus, consisting of two 50 by 10 cm open arms and two 50 by 10 cm closed arms facing each other with a 10 cm square open area and allowed to explore for 15 min. Time spent in either the closed arms or open arms as well as total distance traveled were recorded (Ethovision XT, Noldus). An independent *t*-test was used to analyze data.

Novel Object

Rats were acclimated to a 100 cm square open field box with two inanimate objects placed at equidistant locations for 5 min (two 20 cm tall clear weighted plastic cylinders; 3–4 months of age, AS *n* = 19 (10M, 9F), WT *n* = 15 (7M, 8F). This exploration was repeated after 30 min. One hour after the second exploration, rats were placed back into the same chamber with one of the objects being replaced for a novel object (20 cm tall white glass weighted cuboid-shaped container) and their exploration recorded for 5 min. Twenty-four hours later, the animals were again recorded for 5 min in the box with one familiar (clear cylinder) and a third unfamiliar object (~20 cm tall pink weighted plastic cuboid-shaped object). General activity levels as well as interaction times with the objects were evaluated by video tracking software (Ethovision XT, Noldus). The results are presented as discrimination index which is calculated as (time spent exploring the novel object minus time exploring the familiar)/(total time exploring both novel + familiar) [Antunes & Biala, 2012]. Derived index scores, such as the discrimination index, correct for individual differences in total exploration. A one-way ANOVA was used to analyze data.

Social Approach

Rats were exposed to a 100 cm square three-chamber sociability apparatus (Noldus) containing empty wire cages in the corners of each of the lateral chambers similar to previously described methods [Ku, Weir, Silverman, Berman, & Bauman, 2016; Yang, Silverman, & Crawley, 2011]. Rats at 3–4 months of age (AS male *n* = 6, AS female *n* = 10, WT male *n* = 9, WT female *n* = 6) were acclimated to the device for two trials lasting 5 min with a 15 min inter-trial interval. On the third trial, a novel rat was placed in one of the wire cages. To avoid any distress vocalizations from the novel rat, which could alter tests

results, the novel rat was trained in the wire cage 24 hr before the test. This consisted of placing the animal in the wire cage three times for 30 min each separated by 30 min. The test subject explored the chamber on the third trial for 5 min and the duration of time spent with nose engaged within 5 cm of the novel rat was recorded (Ethovision XT, Noldus). An independent *t*-test was used to analyze data.

Y-Maze

Y-maze was used to assess hippocampal-dependent spontaneous alternation. Rats were placed in an apparatus containing three concentric arms (50 cm) and allowed to explore for 8 min (3–4 months of age, AS *n* = 11 (4M, 7F), WT *n* = 15 (9M, 6F)). Number of alternations (visits to each of the three arms in various orders), arm entries and number of errors (number of direct re-visits or indirect re-visits were recorded using video tracking software (Ethovision XT, Noldus). An independent *t*-test was used to analyze data.

Fear Conditioning

A one-shock associative fear conditioning test was performed to assess hippocampal- and amygdala-dependent learning and memory. The first day consisted of a training phase in which the animal explored a 25 cm square chamber containing a wire grid under bright lighting (Stoelting). This chamber was located inside a sound attenuation chamber. A 5-dB white noise was present inside the chamber during training and contextual conditioning. After 3 min of exploration, rats were presented with a 1,000 Hz, 95 dB tone for 30 sec before receiving a mild foot shock (1.0 mA) at the last 2 sec of the tone. Rats remained in the chamber for an additional 3 min before being placed back in an empty cage and then returned to the colony after all testing was completed. Freezing was recorded as a measure of fear and was designated as a lack of movement for 2 consecutive sec by Ethovision XT software (Noldus). The second phase consisted of contextual and cued conditioning, which took place 72 hr post-training. Rats were placed back into the chamber, but were not exposed to any aversive stimuli, and the animals were monitored for 6 min. One hour following contextual testing, animals were exposed to cued conditioning. The apparatus environment was altered; changing the walls, floor, scent, lighting, as well as the clothes and scent of handler. Rats were placed into this novel context and allowed to habituate for 3 min. Following habituation, the same tone presented in training was administered for 3 min and freezing behavior recorded. Test rats were 3–4 months of age with AS *n* = 11 (5M, 6F) and WT *n* = 14 (7M, 7F). A two-way ANOVA was used to analyze both training and cued fear conditioning and an

independent *t*-test was used to analyze contextual fear conditioning.

Statistics Data was assessed for outliers, by group, prior to analysis. All values exceeding a minimum criteria of 2 standard deviations from the group mean were removed from subsequent analysis. An alpha of 0.05 was used for all main effects. Family-wise error for complex effects was controlled using Tukey's tests. Results are presented as mean ± SEM. For behavioral tests comparing genotypes, an independent *t*-test was used. For behavioral tests being compared over multiple times, a repeated measures ANOVA was used. Statistical analysis was performed using SPSS software or GraphPad Prizm software.

Results

Generation of Ube3a Deletion Rat Model

The CRISPR/Cas9 system was utilized to generate a full deletion of the rat *Ube3a* allele, on chromosome one. To increase the potential for deletion of the entire *Ube3a* gene, four guide RNAs were designed to flank the entire *Ube3a* genomic region, two at each end of the gene. To facilitate the deletion, an additional vector containing arms of homology spanning the targeted region, were included and sequence verified. To confirm deletion of the targeted region, PCR was performed, probing DNA with primers spanning the deleted region. These primers annealed upstream of the 5′ CRISPR cut site and downstream of the 3′ CRISPR cut site. This identified two positive hits. However, these primers did not account for random insertion of the vector containing homology regions. Therefore, a second set of primers that span the deleted region, but anneal outside of the vector arms was used to confirm deletion. This confirmed the identification of the two deletion animals. The offspring positive for the entire deletion were used as the founder line. The founder rats were bred with an outbred CD® (Sprague Dawley) IGS rat colony (Charles River) to obtain heterozygous offspring. After confirmation of the first generation having the entire *Ube3a* gene deleted, studies began utilizing the second-generation rats. Although both rats generated a large deletion of ~90 Kbp, there was a small difference of ~20 bp between the two founders. This study focused on characterizing the rat founder shown in Figure 1A.

Breeding Ability and Observational Behavior

Male founder rats were bred to obtain paternal deletion offspring. Female offspring carrying the *Ube3a* deletion were then bred with Sprague–Dawley males to produce maternal deletion offspring for experiments. A comparison of the offspring from dams that had a paternal deletion or maternal deletion demonstrated they both had
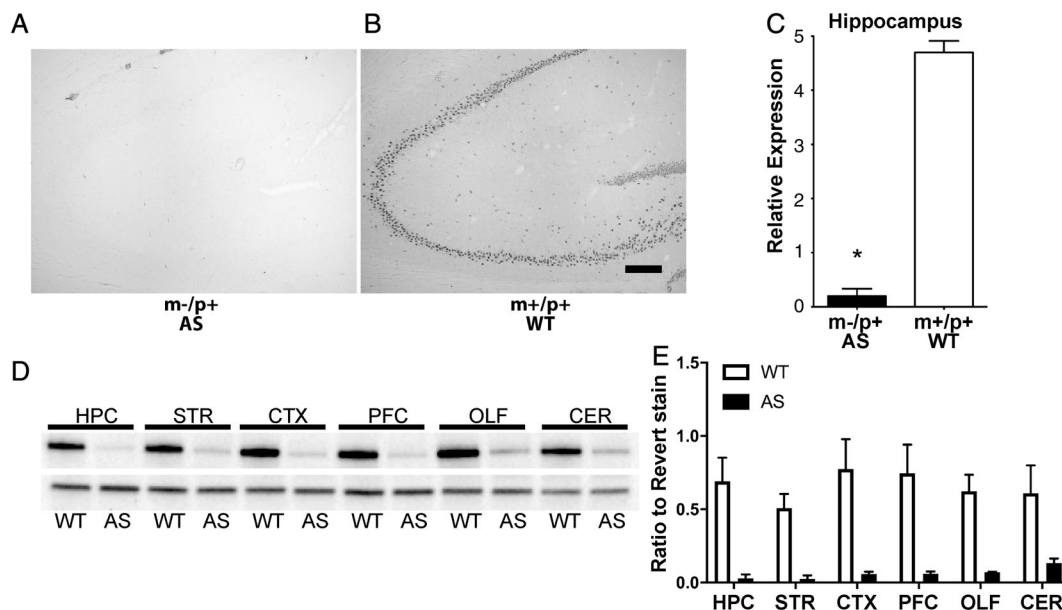
Figure 2. Characterization of *Ube3a* deletion rat CNS. (A) Representative anti-E6AP immunohistochemical images of the hippocampus of AS and WT brains showing little to no E6AP detected in the AS rat brain. There were also no obvious gross anatomical aberrations between groups. Scale bar = 200 μm. (B) Relative anti-E6AP staining for the rat hippocampus shows a significant reduction in E6AP staining (AS *n* = 10 (5M, 5F); WT *n* = 10 (5M, 5F); *t*(18) = 17.88, *P* < 0.05). (C) Western blot with anti-E6AP antibody demonstrating a significant and near-complete reduction of Ube3a within various brain regions. (D) Quantitation of western blot panel C (relative to total protein from Revert staining). HPC, hippocampus; STR, striatum; PFC, prefrontal cortex; CX, rest of cortex; CER, cerebellum; OLF, olfactory bulbs.

normal breeding ability with no differences in litter sizes and Mendelian distribution (Fig. 1D). Therefore, maternal deletion females were used for breeding to generate AS animals without the need to maintain a paternal inherited dam line.

Animal weight was examined from day 21 (weaning) until 1 year of age. We observed no differences in weight gain between the AS animals and their littermate controls (Fig. 1E). This is contrary to the mouse model where AS mice show significant weight gain. It should be noted that AS patients do not typically demonstrate excess weight gain like mice, thus the rat more closely emulates the patient condition [Clayton-Smith & Laan, 2003; Williams, 2010].

To establish a baseline of behavior of the AS rats we performed a functional observational battery. We examined arousal, cage crosses, grooming behavior, overall eating and drinking, and total fecal and urine spot counts. There were no significant differences in these home-cage observational studies between all the groups of rats tested, which included a comparison of male (m−/p+ and m+/p+) and female (m−/p+ and m+/p+) animals.

Expression of Ube3a in Maternal-Deficient Model

Studies began by analyzing overall gross brain structure. Within the human AS population, there are no obvious gross anatomical defects although some patients exhibit microcephaly [Bird, 2014; Williams et al., 2010]. When looking at overall gross structure of the rat brain, there are no obvious anatomical aberrations in the brain when comparing adult maternal-deficient rats and wild-type littermate controls at 4 months of age.

To confirm the reduction in E6AP protein expression in the AS rat we examined homogenized tissue from the CNS by western blot analysis (Figs. 2D and 2E). As stated above, biallelic expression is seen in mammalian peripheral tissues,
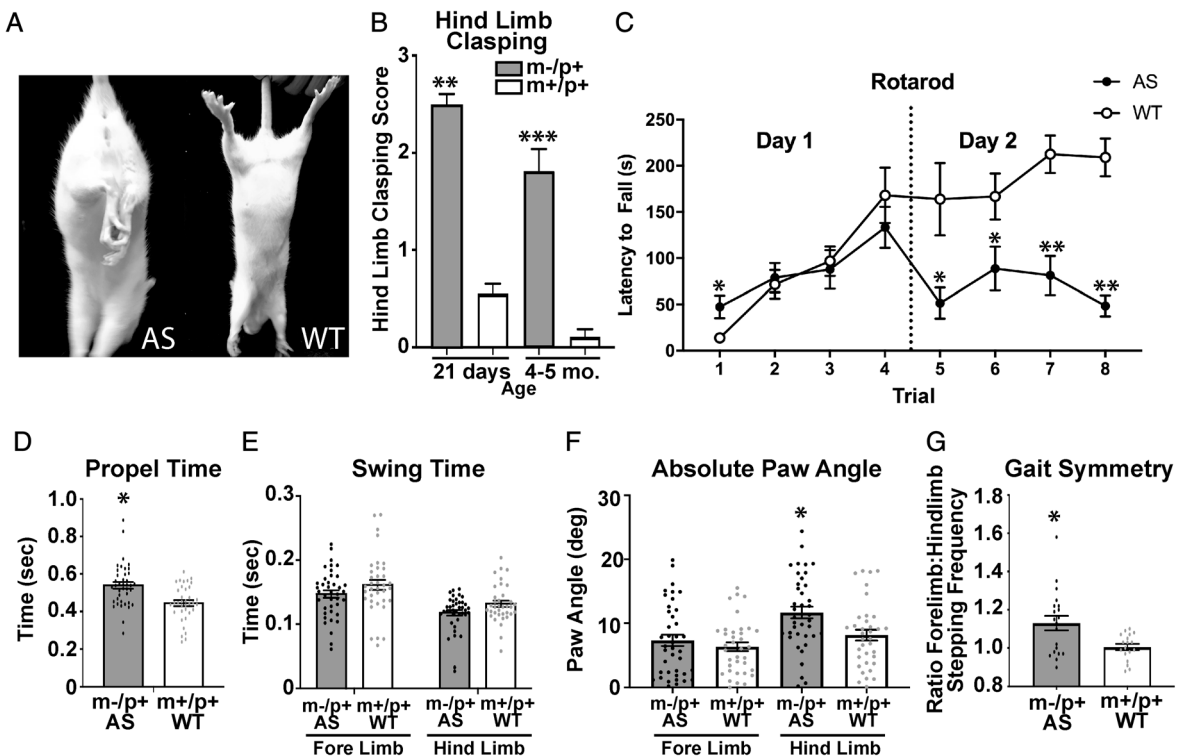
Figure 3. AS rats exhibit hind limb clasping and alterations in gait. (A) Representative limb postures following tail suspension in both AS and WT rats (4 weeks post-natal). (B) AS (21 days $n = 69$ (30F, 39M), 4–5 months $n = 16$ (8F, 8M)) display a significant increase in hind limb clasping compared to WT (21 days, $n = 90$ (45F, 45M), 4–5 months $n = 11$ (8F, 10M)) (21 days, $t(157) = 13.03$, *$P < 0.001$, 4–5 months, $t(32) = 7.43$, $p < 0.0001$). (C) AS rats display decreased latency to fall off of rotating rod ($n = 10$) during trials 1, 5, 6, 7, and 8. (AS $n = 10$ (5M, 5F), WT $n = 10$ (5M, 5F); $F(7,126) = 9.989$, $P < 0.0005$. (D) AS rats display decreased hind limb propel time (time required for accelerating the motion and continuing the forward motion) when compared to WT littermate controls (AS $n = 20$ (11F, 9M), WT $n = 18$ (8F, 10M); $t(74) = 3.908$, *$P < 0.0005$). (E) There are no significant differences between groups in swing time (time duration of swinging the paw without belt contact; Swing fore-limb $t(74) = 1.455$, $P > 0.05$; Swing hind-limb $t(74) = 2.13$, $P > 0.05$). (F) Significant differences were observed between groups in paw angle (absolute degree of paw angle) (paw angle fore-limb $t(74) = 0.865$, $P > 0.05$; paw angle hind-limb $t(74) = 2.217$, $P < 0.007$). (G) AS rats display an alteration in gait symmetry when compared to WT littermate controls ($t(36) = 2.919$, $P < 0.007$) (gait symmetry: ratio of fore limb stepping frequency to hind limb stepping frequency). All outliers that were excluded from analysis (greater than 2 standard deviations from mean) are indicated by a square rather than a circle.

but in neurons *Ube3a* expression predominately arises *via* the maternal allele due to the paternal allele imprinting. As expected, there is almost complete absence in protein expression in all CNS regions tested (Fig. 2). Immunohistochemical staining of the rat brains for E6AP shows little to no E6AP staining in the AS animals compared to the wild-type littermate control animals (Figs. 2A–2C).

General Locomotor Ability

Locomotor aberrations or ataxia are a prominent phenotype within the human AS population as well as in AS mouse models [Grieco, Gouelle, & Weeber, 2018; Y. H. Jiang et al., 1998; Williams, 2010; Williams et al., 2010]. Hind limb clasping has been used as an indicator of cerebellar ataxia and is an established phenotype in the AS mouse [Lalonde & Strazielle, 2011; Mandel-Brehm, Salogiannis, Dhamne, Rotenberg, & Greenberg, 2015]. The maternal-deficient rats recapitulate this phenotype seen in the AS mice, displaying a significant increase in hind limb clasping compared to wild-type littermates (Figs. 3A and 3B). This could suggest a cerebellar ataxia phenotype.

We sought to determine if the ataxia extended to motor coordination and motor learning. The AS mouse model has demonstrated a significant deficit in rotarod leading us to expect a similar deficit in the AS rat. On day 2 of rotarod, the AS rats displayed a significant deficit in motor skills learning compared to wild-type littermates in latency to fall off the accelerating rod (Fig. 3C).

To examine the AS rats gait in more detail, we used the DigiGait. This system allows quantification of both spatial and temporal gait parameters while the rats are walking on a translucent, motorized treadmill. These parameters include propel time, being defined as the time required to accelerate the motion and continuing that motion forward. When an animal exhibits a shorter duration in propel time, they display a greater strength and better control in accelerating that motion. The AS rats exhibit a higher score than the wild-type littermates, indicating they have less strength and less control in their propel ability (Fig. 3D). Another parameter examined was swing time, being defined as the duration of swinging the paw while walking without making contact on the belt of the treadmill. There were no significant
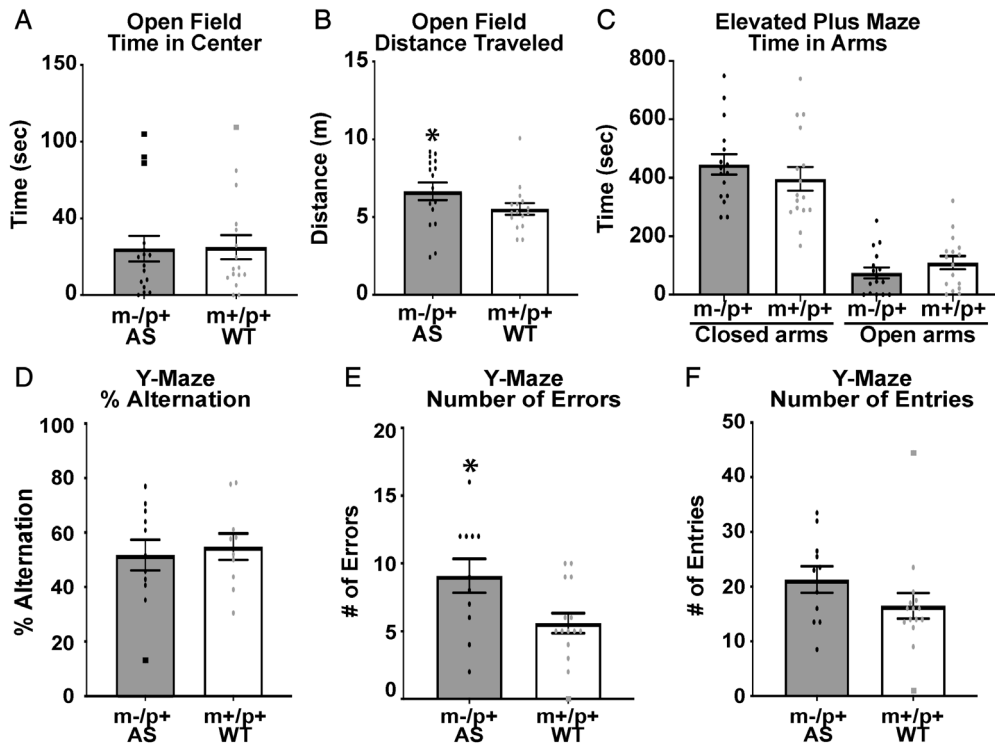
Figure 4. AS rats do not demonstrate an anxiety phenotype but have a deficit in learning and memory. (A) No differences in time spent in center of open field chamber (AS $n = 16$ (8M, 8F), WT $n = 16$ (8M, 8F), $t(26) = 1.4$, $P > 0.17$). (B) There was a significant difference between groups in total distance traveled in open field ($t(29) = 2.295$, $P < 0.05$)). (C) No differences were observed in elevated plus maze testing (AS $n = 16$ (8M, 8F), WT $n = 16$ (8M, 8F), time in closed arms $t(30) = 0.926$, $P > 0.36$, time in open arms $t(30) = 1.17$, $P > 0.09$). (D) AS rats did not display a significant difference in percent alternations in the Y-maze (AS $n = 11$ (4M, 7F), WT $n = 15$ (9M, 6F) ($t(23) = 0.217$, $P > 0.77$). (E) AS rats displayed a significant increase in the number of total errors made within the Y-maze ($t(23) = 2.295$, $P < 0.05$). (F) AS rats showed no difference in the number of arm entries ($t(23) = 1.19$, $P > 0.27$). All outliers that were excluded from analysis (greater than 2 standard deviations from mean) are indicated by a square rather than a circle.

differences between groups in swing time (Fig. 3E). There was, however, a significant increase in the hind limb paw angle, indicating that the AS rats placed their hind limbs at a more lateral-facing position (Fig. 3F). This finding relates well with an increase in propel time in that typical paw angles require less propel time, as seen in the wild-type littermates. Finally, gait symmetry was assessed. This is a ratio of forelimb stepping frequency to hind limb stepping frequency. There was a significant difference with the AS rats having an elevated stepping frequency when compared to wild-type littermates (Fig. 3G). A gait symmetry level of 1 indicates a 1:1 stepping frequency between fore and hind limbs. These data demonstrate that the AS rat has a deficit in hind limb coordination.

To examine general locomotor activity and to examine for any anxiety phenotype, we employed the open field [Denenberg, 1969], light/dark [Arrant, Schramm-Sapyta, & Kuhn, 2013], and elevated plus maze behavioral tasks [Pellow, Chopin, File, & Briley, 1985]. We found the AS rats do not have a significant difference in the light–dark test compared to wild-type littermates (data not shown). Consistent with this, we observed no differences in time spent in the open arms in elevated plus maze (Fig. 4C). There were no significant differences in time spent in the center of the open field (Fig. 4A). These results suggest that these animals do not display an obvious anxiety phenotype. In distance traveled in the open field, we did observe a significant increase compared to wild-type littermates, suggesting a possible hyperactive phenotype (Fig. 4B).

Learning and Memory

Hippocampal-dependent spontaneous alternation and associative learning and memory testing were performed using the Y-maze and fear conditioning. For Y-maze, animals were placed in the apparatus for 8 min. Arm entries and alternations were recorded as well as total number of errors. Although there were no differences observed in
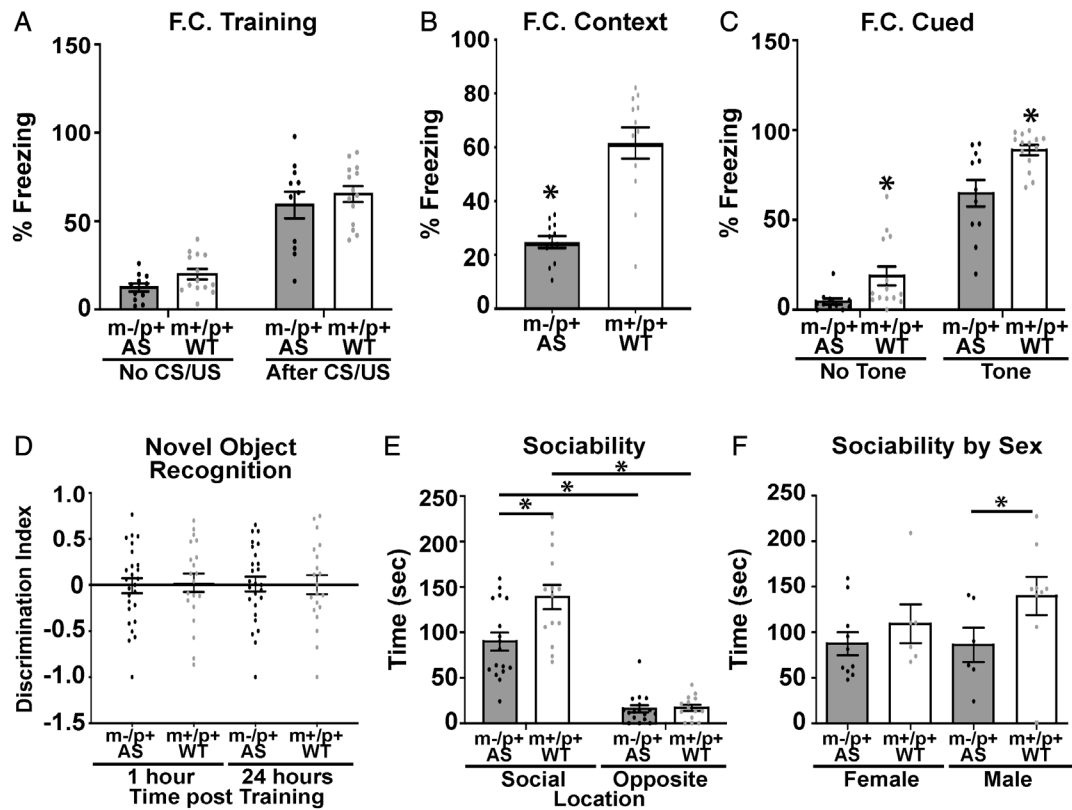
Figure 5. AS rats display deficits in hippocampal-dependent learning and memory. (A) AS rats showed no significant difference in percent freezing during fear conditioning training (AS $n = 11$ (5M, 6F), WT $n = 14$ (7M, 7F); $F_{(1,23)} = 0.0165$, $P > 0.05$). (B) AS rats show a significant deficit in percent of time freezing 72 hr post-training during context testing ($t_{(23)} = 5.054$, $P < 0.0002$. (C) AS rats displayed a deficit in cued fear conditioning 72 hr post-training ($F_{(1,23)} = 263$, $P < 0.002$). (D) Novel object recognition showed no significant differences in discrimination index with wild type controls (AS $n = 19$ (10M, 9F), WT $n = 15$ (7M, 8F)) ($F_{(3,88)} = 0.03$, $P > 0.05$). (E) All animals exhibited preference for the novel rat compared to the opposite, empty cage, but AS rats showed reduced interaction with the novel target rat compared to WT rats (AS $n = 16$ (6M, 10F), WT $n = 15$ (9M, 6F)) ($F_{(1,29)} = 12.53$, $P < 0.002$). (F) This reduction in interaction was predominantly due to the male AS rats (AS $n = 16$ (6M, 10F), WT $n = 15$ (9M, 6F)) ($t_{(12)} = 3.186$, $P < 0.008$). All outliers that were excluded from analysis (greater than 2 standard deviations from mean) are indicated by a square rather than a circle.

alternations, there was a significant increase in the number of errors in the AS rats compared to their wild type littermates (Figs. 4D–4F).

Contextual and cued fear conditioning were performed to assess hippocampal-dependent associative learning and memory. A one foot-shock paradigm followed by a 72-hr post-training contextual and cued test were utilized for this portion. No significant differences were observed during fear conditioning training (Fig. 5A). However, 72 hr post-training, the AS rats have deficits in both cued and contextual fear conditioning (Figs. 5B and 5C). AS mice show a strain-dependent deficit in contextual or cued freezing [Born et al., 2017; Huang et al., 2013; Y. H. Jiang et al., 1998].

Rats were tested in novel object recognition. Both WT and AS rats were tested 1 and 24 hr after training with different novel objects to test their recognition memory. It was found that the AS rats have no significant deficits in short or long-term object recognition memory compared with wild-type littermates according to their discrimination index: ((Time(novel) − Time(familiar))/(Time/novel + familiar)) (Fig. 5D).

Social approach studies using an AS mouse model are complicated by strain differences. AS 129 mice had low activity making assessment difficult, while B6 AS mice had reduced exploration during the social approach testing but no significant deficits in social approach [Allensworth, Saha, Reiter, & Heck, 2011; Huang et al., 2013]. Interestingly the FVB AS mice (back-crossed into FVB) demonstrated an increase in social interactions with a novel mouse [Stoppel & Anderson, 2017]. Therefore, we examined the rats in a social approach test. We observed that the AS rats had an increased preference for interacting with the novel rat compared to the empty chamber, but this interaction was significantly reduced compared to the wild-type littermates (Fig. 5E), suggesting a deficit in social interaction in the AS rat compared to the wild type littermate. However, a comparison of sex differences in this task, demonstrated that the differences we observed in this task are predominantly due to a significant difference in male AS rats compare to the wild type littermates, with no significant difference seen in the females (Fig. 5F).

Discussion

Using the CRISPR/Cas9 system we have created a maternal *Ube3a* deletion AS rat model resembling many of the deficits manifested in human AS, as well as the highly characterized AS mouse model. This rat model displays normal breeding ability, litter number, and Mendelian distribution. There have been many notable challenges with the current AS mouse model such as, but not limited to, strain dependency and loss of phenotype over time

[Born et al., 2017; Huang et al., 2013]. This has led to a high demand for a more phenotypically consistent AS animal model which better resembles the human condition. The AS mouse model was created by a null mutation of exon 2 on the maternal *Ube3a* gene. This mutation encompasses a small subset of the genetic alterations that lead to the manifestation of human AS (~13%), while the majority of human AS cases (~70%) are due to a large deletion within maternal chromosome 15 q11-13 including the complete deletion of the *UBE3A* gene [Y. Jiang et al., 1999; Lalande & Calciano, 2007]. In our rat model, we generated a deletion of the entire maternal *Ube3a* gene. We have demonstrated that this model has a pervasive deletion of the maternal Ube3a gene in the CNS. The remaining low levels that are detected *via* western blotting are believed to be contributed by glial cell expression, which is similar to the mouse model [Yamasaki et al., 2003]. Additionally, we did not observe any obvious gross anatomical changes, as previously observed in the mouse model. The AS rat model is genetically similar to most human AS cases demonstrating deficits in UBE3A within the CNS. Given that our novel rat model genetically recapitulates AS, demonstrating a deficit in Ube3a expression, we sought to determine if it also displayed hallmark deficits in motor coordination tasks. There have been no reports indicating a sex difference within the human population of AS or within the AS mouse models. We chose to analyze sex differences in behaviors to ensure there are no differences within the AS rat. We analyzed differences in rotarod, open field, elevated plus maze, and DigiGait and there were no sex differences in any test. However, within social approach sex is a confounding variable in wild type animals. At the age of the animals tested, there may be a difference in motivation for males *versus* female rats. Considering this, we examined for sex differences within social approach. No differences were observed between AS and WT females but there was a significant difference between AS and WT males, with AS males showing reduced interaction.

Motor coordination deficits are a hallmark phenotype associated with human AS. Hind limb clasping has been a well-documented phenotype associated with the AS mouse model and has been shown to be indicative of cerebellar ataxia as well as anxiety. Our rat model displayed prominent hind limb clasping as opposed to wild-type littermates. This phenotype was present at an early age and persisted into adulthood. To ensure that the increase in hind limb clasping is not due to an increase in anxiety, we performed the light/dark behavioral task. We found that the AS rat did not show increased anxiety in the light/dark task when compared to WT controls. Similarly, we did not observe any indications of an anxiety phenotype in open field or elevated plus maze. This suggests that the significant difference in hind limb clasping is likely due to an ataxic phenotype.

We next evaluated this potential cerebellar deficit on the rotarod task, as motor deficits are a hallmark phenotype in the AS mouse model. Like the AS mouse, we observed a significant deficit in rotarod performance. It is worth noting that the AS mouse model shows a significant increase in weight as they age compared to wild-type mice [Ciarlone, Grieco, D'Agostino, & Weeber, 2016]. Increased weight gain is only seen in a small subset of the human population [Clayton-Smith & Laan, 2003; Williams, 2010]. It is unknown if the weight gain in the AS mice is a significant confound in the rotarod causing the mice to inaccurately demonstrate a deficit in motor coordination. However, our AS rat model does not show a difference in weight gain from the wild-type littermates, yet still demonstrated a significant deficit in rotarod performance. This suggests that the rotarod deficits seen in both models are likely due to an ataxic phenotype, thus recapitulating the disease phenotype in humans. The weight gain in the AS mice may confound other tasks such as open field distance traveled. It has been reported that in certain strains of AS mice there is a significant reduction in distance traveled [Born et al., 2017; Huang et al., 2013], but with the AS rats we observed a significant increase in distance traveled, suggesting a more hyperactive phenotype. Hyperactive behaviors have been reported in the human AS condition [Williams et al., 2010].

We also evaluated motor function using DigiGait, which can more closely analyze gait parameters which rotarod cannot. Examination of spatiotemporal parameters in AS patients walking demonstrated that the AS children exhibited shorter step length, decreased cadence and consequently lower speed, higher stride width, and less time spent in single support compared to neurotypical children [Grieco et al., 2018]. We were able to determine that the AS rat model has significant alterations in gait compared to wild-type littermates. We observed an increase in propel time which is an indication of reduced strength and control of movements. The AS rats also had an alteration in hind limb paw angle. Paw angle is also known as degree of external rotation, thigh-foot angle (in people), toe in/out angle (in people), or splay angle. The AS rats displayed an increase in paw angle indicative of an increased splaying of the hind paws. More open angles of the hind paws are associated with ataxia, spinal cord injury, and demyelinating disease [Powell, Anch, Dyche, Bloom, & Richtert, 1999]. An examination of gait symmetry (a ratio of fore limb stepping to hind limb stepping) showed a significant increase, suggesting a reduction in hind limb movement compared to the fore limbs. These DigiGait data imply that the AS rat motor deficit is likely due to a problem in hind limb coordination and control. Thus, the AS rat can model the deficits in motor coordination that are commonly reported in the AS population. This could be a useful outcome measure for testing therapeutics that could improve the motor deficits in AS.

The AS rat showed deficits in standard learning and memory tasks. Compared to wild-type littermate controls we observed increases in the number of errors in Y-maze, as well as a deficit in the fear conditioning task. We did not observe a difference in novel object recognition, which has previously been reported for some AS mouse strains but not all [Born et al., 2017; Huang et al., 2013]. Contextual fear conditioning deficits are also strain dependent, with 129 mice but not B6 mice exhibiting deficits [Born et al., 2017; Huang et al., 2013]. Typically there is not a deficit in cued fear conditioning in AS mice [Born et al., 2017; Daily et al., 2011] but one group has reported a deficit in B6 mice [Huang et al., 2013], suggesting that this phenotype is not consistent in the AS mouse, which confounds its use especially between labs. Interestingly, we observed deficits in both the contextual and cued responses in the fear conditioning task with the AS rat. The hippocampal-dependent contextual deficit is greater than the cued deficit, as may be expected from mouse studies, but the cued deficit present in the rat could exemplify the greater complexity of the rat which allows more subtle deficits to become apparent. This suggests that the AS rat may offer a better model for studying therapeutic interventions for AS. Further investigation is required to examine aspects of learning and memory such as hippocampal synaptic plasticity through long-term potentiation and long-term depression in these animals.

Although inbred strains offer genetic uniformity, the outbred stocks, known for genetic variability are often used to potentially more closely mimic what one would find in the human population. We used the outbred Sprague–Dawley rats with the goal to represent more diversity and thus hopefully more translatability to the human AS population. As discussed above, there are many advantages to using a rat model over a mouse model to mimic a human disorder, including its genetic similarity (90% of rat genes possess strict orthologues of the human genes [Gibbs, et al., 2004]) and its closer resemblance to human physiology. The rat has a much higher level of complexity within its physiological systems, more accurately reflecting human physiology than mice [Iannaccone & Jacob, 2009]. One example of this is Melatonin, an important mediator for complex physiological functions including circadian regulation, sleep, and cognition (which are all disrupted in AS). Most inbred mouse strains, including, C57BL/6, have been reported to be deficient in melatonin, while rats similar to humans produce this hormone [Ebihara, Marks, Hudson, & Menaker, 1986; Korf, Von Gall, & Stehle, 2003; Roseboom et al., 1998; Stehle, von Gall, & Korf, 2002]. This can make the rat a much more relevant model for neuropsychiatric disorders.

The creation of a novel AS model more accurately depicting the human condition was in high demand and with advances in CRISPR/Cas9, we have been able to create such a model. We have generated a novel AS rat which we believe recapitulates many aspects of AS, including significant deficits in motor coordination (rotarod, DigiGait, hind-limb clasping) and learning (cued and contextual fear conditioning). Although a robust deficit was observed in fear conditioning, other memory tasks such as Y-maze and novel object recognition did not show significant differences to wildtype rats, demonstrating the sensitive nature of learning and memory deficits in rodent models. This new model should offer avenues for increased exploration of AS and advance our understanding of molecular targets of Ube3a thus expanding our knowledge of the disease. This model offers a high potential utility for drug evaluation, biomarker discovery, and will aid in the development and testing of novel therapeutic treatments. The rat would offer a model to test both efficacy and toxicology within one animal model.

Acknowledgments

Conflict of Interest

The authors declared that they have no conflicts of interest.

References

Allensworth, M., Saha, A., Reiter, L. T., & Heck, D. H. (2011). Normal social seeking behavior, hypoactivity and reduced exploratory range in a mouse model of Angelman syndrome. BMC Genetics, 12, 7.

Antunes, M., & Biala, G. (2012). The novel object recognition memory: neurobiology, test procedure, and its modifications. Cognitive Processing, 13, 93–110.

Arrant, A. E., Schramm-Sapyta, N. L., & Kuhn, C. M. (2013). Use of the light/dark test for anxiety in adult and adolescent male rats. Behavioural Brain Research, 256, 119–127.

Bird, L. M. (2014). Angelman syndrome: review of clinical and molecular aspects. The Application of Clinical Genetics, 7, 93–104.

Born, H. A., Dao, A. T., Levine, A. T., Lee, W. L., Mehta, N. M., Mehra, S., … Anderson, A. E. (2017). Strain-dependence of the Angelman Syndrome phenotypes in Ube3a maternal deficiency mice. Scientific Reports, 7, 8451.

Ciarlone, S. L., Grieco, J. C., D'Agostino, D. P., & Weeber, E. J. (2016). Ketone ester supplementation attenuates seizure activity, and improves behavior and hippocampal synaptic plasticity in an Angelman syndrome mouse model. Neurobiology of Disease, 96, 38–46.

Clayton-Smith, J., & Laan, L. (2003). Angelman syndrome: a review of the clinical and genetic aspects. Journal of Medical Genetics, 40, 87–95.

Daily, J. L., Nash, K., Jinwal, U., Golde, T., Rogers, J., Peters, M. M., … Weeber, E. J. (2011). Adeno-associated virus-mediated rescue of the cognitive defects in a mouse model for Angelman syndrome. PLoS One, 6, e27221.

Denenberg, V. H. (1969). Open-field bheavior in the rat: What does it mean? Annals of the New York Academy of Sciences, 159, 852–859.

Ebihara, S., Marks, T., Hudson, D. J., & Menaker, M. (1986). Genetic control of melatonin synthesis in the pineal gland of the mouse. Science, 231, 491–493.

Ellenbroek, B., & Youn, J. (2016). Rodent models in neuroscience research: is it a rat race? Disease Models & Mechanisms, 9, 1079–1087.

Gibbs, R. A., Weinstock, G. M., Metzker, M. L., Muzny, D. M., Sodergren, E. J., Scherer, S., … Rat Genome Sequencing Project Consortium. (2004). Genome sequence of the Brown Norway rat yields insights into mammalian evolution. Nature, 428, 493–521.

Grieco, J. C., Gouelle, A., & Weeber, E. J. (2018). Identification of spatiotemporal gait parameters and pressure-related characteristics in children with Angelman syndrome: A pilot study. Journal of Applied Research in Intellectual Disabilities, 31, 1219–1224.

Gustin, R. M., Bichell, T. J., Bubser, M., Daily, J., Filonova, I., Mrelashvili, D., … Haas, K. F. (2010). Tissue-specific variation of Ube3a protein expression in rodents and in a mouse model of Angelman syndrome. Neurobiology of Disease, 39, 283–291.

Huang, H. S., Burns, A. J., Nonneman, R. J., Baker, L. K., Riddick, N. V., Nikolova, V. D., … Moy, S. S. (2013). Behavioral deficits in an Angelman syndrome model: effects of genetic background and age. Behavioural Brain Research, 243, 79–90.

Iannaccone, P. M., & Jacob, H. J. (2009). Rats! Disease Models & Mechanisms, 2, 206–210.

Jiang, Y., Lev-Lehman, E., Bressler, J., Tsai, T. F., & Beaudet, A. L. (1999). Genetics of Angelman syndrome. American Journal of Human Genetics, 65, 1–6.

Jiang, Y. H., Armstrong, D., Albrecht, U., Atkins, C. M., Noebels, J. L., Eichele, G., … Beaudet, A. L. (1998). Mutation of the Angelman ubiquitin ligase in mice causes increased cytoplasmic p53 and deficits of contextual learning and long-term potentiation. Neuron, 21, 799–811.

Judson, M. C., Burette, A. C., Thaxton, C. L., Pribisko, A. L., Shen, M. D., Rumple, A. M., … Philpot, B. D. (2017). Decreased Axon Caliber Underlies Loss of Fiber Tract Integrity, Disproportional Reductions in White Matter Volume, and Microcephaly in Angelman Syndrome Model Mice. The Journal of Neuroscience, 37, 7347–7361.

Korf, H. W., von Gall, C., & Stehle, J. (2003). The circadian system and melatonin: lessons from rats and mice. Chronobiology International, 20, 697–710.

Ku, K. M., Weir, R. K., Silverman, J. L., Berman, R. F., & Bauman, M. D. (2016). Behavioral Phenotyping of Juvenile Long-Evans and Sprague–Dawley Rats: Implications for Preclinical Models of Autism Spectrum Disorders. PLoS One, 11, e0158150.

Kummer, K. K., Hofhansel, L., Barwitz, C. M., Schardl, A., Prast, J. M., Salti, A., … Zernig, G. (2014). Differences in social interaction- vs. cocaine reward in mouse vs. rat. Frontiers in Behavioral Neuroscience, 8, 363.

Lalande, M., & Calciano, M. A. (2007). Molecular epigenetics of Angelman syndrome. Cellular and Molecular Life Sciences, 64, 947–960.

Lalonde, R., & Strazielle, C. (2011). Brain regions and genes affecting limb-clasping responses. Brain Research Reviews, 67, 252–259.

Mandel-Brehm, C., Salogiannis, J., Dhamne, S. C., Rotenberg, A., & Greenberg, M. E. (2015). Seizure-like activity in a juvenile Angelman syndrome mouse model is attenuated by reducing Arc expression. Proceedings of the National Academy of Sciences of the United States of America, 112, 5129–5134.

Meng, L., Person, R. E., & Beaudet, A. L. (2012). Ube3a-ATS is an atypical RNA polymerase II transcript that represses the paternal expression of Ube3a. Human Molecular Genetics, 21, 3001–3012.

Moser, V. C., & MacPhail, R. C. (1992). International validation of a neurobehavioral screening battery: the IPCS/WHO collaborative study. Toxicology Letters, *64–65 Spec No*, 64-65, 217–223.

Parasuraman, S. (2011). Toxicological screening. Journal of Pharmacology and Pharmacotherapeutics, 2, 74–79.

Pellow, S., Chopin, P., File, S. E., & Briley, M. (1985). Validation of open:closed arm entries in an elevated plus-maze as a measure of anxiety in the rat. Journal of Neuroscience Methods, 14, 149–167.

Powell, E., Anch, A. M., Dyche, J., Bloom, C., & Richtert, R. R. (1999). The splay angle: A new measure for assessing neuromuscular dysfunction in rats. Physiology & Behavior, 67, 819–821.

Roseboom, P. H., Namboodiri, M. A., Zimonjic, D. B., Popescu, N. C., Rodriguez, I. R., Gastel, J. A., & Klein, D. C. (1998). Natural melatonin "knockdown" in C57BL/6J mice: rare mechanism truncates serotonin N-acetyltransferase. Brain Research. Molecular Brain Research, 63, 189–197.

Stehle, J. H., von Gall, C., & Korf, H. W. (2002). Organisation of the circadian system in melatonin-proficient C3H and melatonin-deficient C57BL mice: a comparative investigation. Cell and Tissue Research, 309, 173–182.

Stoppel, D. C., & Anderson, M. P. (2017). Hypersociability in the Angelman syndrome mouse model. Experimental Neurology, 293, 137–143.

Sumova, A., Sladek, M., Jac, M., & Illnerova, H. (2002). The circadian rhythm of Per1 gene product in the rat suprachiasmatic nucleus and its modulation by seasonal changes in daylength. Brain Research, 947, 260–270.

Williams, C. A. (2010). The behavioral phenotype of the Angelman syndrome. American Journal of Medical Genetics. Part C, Seminars in Medical Genetics, 154C, 432–437.

Williams, C. A., Beaudet, A. L., Clayton-Smith, J., Knoll, J. H., Kyllerman, M., Laan, L. A., … Wagstaff, J. (2006). Angelman syndrome 2005: updated consensus for diagnostic criteria. American Journal of Medical Genetics. Part A, 140, 413–418.

Williams, C. A., Driscoll, D. J., & Dagli, A. I. (2010). Clinical and genetic aspects of Angelman syndrome. Genetics in Medicine, 12, 385–395.

Yamasaki, K., Joh, K., Ohta, T., Masuzaki, H., Ishimaru, T., Mukai, T., … Kishino, T. (2003). Neurons but not glial cells show reciprocal imprinting of sense and antisense transcripts of Ube3a. Human Molecular Genetics, 12, 837–847.

Yang, M., Silverman, J. L., & Crawley, J. N. (2011). Automated three-chambered social approach task for mice. Current Protocols in Neuroscience, 8, 8.26.